ELSEVIER

Journal of Nuclear Materials 305 (2002) 209–219

journal of nuclear materials

www.elsevier.com/locate/jnucmat

Influence of chemical composition, prior deformation and prolonged thermal aging on the sensitization characteristics of austenitic stainless steels

N. Parvathavarthini, R.K. Dayal *

Aqueous Corrosion and Surface Studies Section, Corrosion Science and Technology Division, Materials Characterisation Group, Indira Gandhi Centre for Atomic Research, Kalpakkam 603102, Tamilnadu, India

Received 13 August 2001; accepted 26 June 2002

Abstract

Sensitization behaviour of austenitic stainless steels are greatly influenced by several metallurgical factors such as chemical composition, degree of prior deformation, grain size, aging temperature–time. The need for generation of data on sensitization kinetics for specific composition of stainless steels to take care of the heat to heat variation for the fabrication of critical components is often questioned. An attempt was made in this investigation to understand this aspect by establishing time–temperature–sensitization diagrams, continuous-cooling–sensitization diagrams and critical cooling rate for three sets of AISI 316 stainless steel in which as the wt% of carbon decreases, that of nitrogen increases so as to encompass the normal span of concentration range usually encountered in different heats. A systematic trend is observed in these experimentally determined sensitization data of these typical stainless steels. This would eliminate the need for the independent generation of sensitization data for stainless steel of specified composition which is within the range investigated here. The database reported for these alloys will also help to recommend the limits of critical cooling rate to avoid sensitization during fabrication.

1. Introduction

Austenitic stainless steels are the most favoured construction materials of various components required in chemical, petrochemical, fertilizer and nuclear industries. The selection of these steels is made basically due to a good combination of mechanical, fabrication and corrosion resistance properties. However, these steels are prone to sensitization when subjected to heating in the temperature range of 723–1123 K. In this phenomenon, usually $(Fe,Cr)_{23}C_6$ precipitation at the grain boundaries and the subsequent chromium depletion adjacent to the precipitates take place. In the sensitized condition, the steels are quite susceptible to intergranular corrosion (IGC) and intergranular stress corrosion cracking (IGSCC) in chloride and caustic environments resulting in premature failures of the fabricated components. The sensitization temperature range is often encountered during isothermal heat treatment of the fabricated components for stress relieving purpose, prolonged service at elevated temperatures, slow cooling from higher temperatures (e.g. solution annealing or during shut down of plant operating at higher temperatures), the improper heat treatment in the heat affected zone (HAZ) of the weldments or hot working of the material.

Sensitization resulting from isothermal exposures is normally represented by time–temperature–sensitization (TTS) diagrams which are plots of aging time versus temperature necessary for sensitization. These are 'C' shaped curves which demarcate sensitized and

* Corresponding author. Fax: +91-4114 480 081.
E-mail address: rkd@igcar.ernet.in (R.K. Dayal).

0022-3115/02/$ - see front matter
PII: S0022-3115(02)00915-7

non-sensitized regions. These diagrams show the duration required for isothermal sensitization at various temperatures and can be used to solve problems such as the choice of conditions of annealing and stress relieving which will not result in sensitization. The nose of this curve specifies the critical temperature at which the time required for sensitization is minimum (t_{min}).

Sensitization may also result from cooling through the sensitization temperature range. This is of great practical importance since it is this type of thermal exposure that occurs in slow cooling after high temperature annealing or during the cooling of a weldment. TTS diagrams do not provide relevant information on the sensitization produced during welding or continuous slow cooling. Dayal and Gnanamoorthy [1] have reported a method to predict the extent of sensitization during continuous cooling/heating of the material. Using this method, critical linear cooling rate (CCR) (above which there is no risk of sensitization) can be calculated from the TTS diagram. Based on the critical cooling rate and TTS diagrams, continuous-cooling–sensitization (CCS) diagrams can be established to determine the sensitization behaviour during continuous cooling/heating.

It is well-established [2] that the degree of sensitization (DOS) is influenced by factors which change the thermodynamics and kinetics of carbide formation at grain boundaries and subsequent chromium depletion (e.g. cold work (CW), grain size, and chemical composition). Although carbon and nitrogen are the predominant compositional variables controlling sensitization kinetics, other alloying elements also influence it by altering carbon and chromium activity. Since minor variations in chemical composition can have significant influence on the sensitization behaviour, quite often question arises as to the need for generation of data on sensitization kinetics for specific composition of stainless steels in order to take care of the heat to heat variation for the fabrication of critical components. To understand this aspect, a critical review of the literature on the influence of chemical composition on the sensitization behaviour was made and it was evident that among the many variants, carbon and nitrogen have predominant influence on the sensitization kinetics. Therefore, three typical alloys were chosen wherein as the concentration of carbon decreases, nitrogen concentration increases so as to encompass the normal span of concentration range usually encountered in 316 stainless steels.

TTS and CCS diagrams and CCR for a nuclear grade AISI type 316 stainless steel used as structural material for fast breeder test reactor at Kalpakkam have been published [3,4] by the authors previously. Similar studies were extended to AISI type 316LN stainless steel which has been proposed as a candidate material for proto type fast breeder reactor at Kalpakkam and the results for this material have also been published [5].

In this paper the results obtained for another alloy whose composition with respect to carbon and nitrogen lies in between the limit set by the above two alloys are presented. Three sets of data from these materials, which were generated by identical experiments in the same laboratory, have facilitated identification of several trends, which were hither to not possible, by scrutinising any one isolated set of data from literature. It is therefore considered that this paper will serve as a data box for analyzing the sensitization behaviour of any structural alloy lying within the range of variations of composition and CW encountered by the designers in their design efforts.

2. Experimental procedure

2.1. Chemical composition

AISI type 316 stainless steel with three different chemical compositions (varying mainly in carbon and nitrogen content) were considered for the present study. The nominal chemical composition of the three steels is given in Table 1. The three alloys are identified as Alloy-1, Alloy-2 and Alloy-3, respectively, in this paper.

2.2. Cold working

The as-received material in mill-annealed condition was taken as reference corresponding to CW of 0%. The as received sheets were cold rolled at ambient temperature to various levels of reduction in thickness ranging from 5% to 25%. Specimens of 100 mm length and 10 mm width with reduced thickness were cut from these cold rolled strips for sensitization testing.

Table 1
Chemical composition (wt%)

Elements	Alloy-1 (AISI 316)	Alloy-2 (AISI 316LN)	Alloy-3 (AISI 316LN)
Carbon	0.054	0.043	0.030
Nitrogen	0.053	0.075	0.086
Chromium	16.46	17.18	16.6
Nickel	12.43	10.23	12.2
Molybdenum	2.28	1.85	2.61
Manganese	1.69	1.54	1.54
Phosphorous	0.025	0.022	0.024
Sulphur	0.006	0.005	0.003
Silicon	0.64	0.585	0.29
Vanadium	–	0.061	0.092
Copper	–	0.207	0.09
Cobalt	–	0.230	–
Boron	–	–	0.0012
Iron	Balance	Balance	Balance
Cr^{eff}	12.57	14.36	16.03

2.3. Heat treatment

The cold worked specimens were heat treated at various temperatures ranging from 773 to 1023 K for duration ranging from 50 to 2000 h. The specimens were air cooled after the heat treatments.

2.4. Specimen preparation

From every cold worked and heat treated specimens, a 10 mm square specimen was cut for performing ASTM A262 practice A test [6]. The balance specimen was used for performing the ASTM A262 practice E [6] test after polishing with successive grades of silicon carbide paper up to 320 grit. The specimens for practice A test were mounted in an epoxy resin (araldite) and were polished up to fine diamond (~3 μm) finish. After polishing, the specimens were washed first with soap solution and then with distilled water and finally they were dried.

2.5. Sensitization test

The specimens were electrolytically etched in 10 wt% ammonium persulphate at a current density of 1 A/cm^2 for 5 min according to ASTM A262 practice A. The etched structure is then examined at 250X and was characterized as step, dual or ditch structure. The specimen showing step or dual structure was considered to be free from sensitization whereas the specimen showing ditch structure was required to be tested further for confirming the presence of sensitization. The specimens were further tested in boiling Cu–H_2SO_4–$CuSO_4$ solution for 24 h according to ASTM A262 practice E. The exposed specimens were bent through 180° over a mandrel of diameter equal to the thickness of the specimen. The bent specimen is examined under low magnification (20×) for appearance of cracks. If cracks are seen, the material is considered to be sensitized.

2.6. Construction of time–temperature–sensitization diagrams

These diagrams were obtained by plotting sensitization tests results on a temperature versus log soaking time axes and drawing a line which demarcates the sensitized and non-sensitized regions.

2.7. Construction of continuous-cooling–sensitization diagrams

From the TTS diagrams, CCS diagrams were obtained for all levels of CW by the method described in the earlier publications [1,4].

2.8. Electrochemical potentiokinetic reactivation test

DOS for several heat treated specimens were also determined using single loop electrochemical potentiokinetic reactivation (EPR) test as described in ASTM standard G108 [6]. This consisted of electrochemical reactivation of specimens at a scan speed of 6 V/h from a passive potential of +200 mV (with respect to a saturated calomel electrode) in 0.5 M sulphuric acid containing 0.01 M ammonium thiocyanate. The reactivation charge density (Q) was calculated from the area under the reactivation peak which is indicative of DOS.

2.9. Phase separation and identification

The specimens which were aged at 898–973 K for 500, 1000 and 2000 h were analyzed for the possible formation of secondary phases. Bulk extraction of the precipitates for XRD studies was carried out by keeping the specimens at 1.5 V with respect to platinum cathode in 10% HCl–90% methanol solution for a duration of 24 h. Austenite phase selectively dissolves and carbides and other secondary phases remain undissolved which were collected by centrifuging. The precipitates were then washed in methanol and dried. Only mill-annealed (0% CW) and 25% CW specimens were subjected to this tests. The extracted powder specimens were characterized by XRD technique using CuK_α radiation.

3. Results and discussion

The TTS and CCS diagrams for Alloy-1 and Alloy-3 in different cold worked conditions were established earlier by the authors [3–5]. The composition of Alloy-2 with respect to carbon and nitrogen lies in between the limit set by Alloy-1 and Alloy-3. Based on the results obtained from A 262 practice E tests in this work, the TTS and CCS diagrams for the Alloy-2 have also been established and are now reported in Figs. 1 and 2, respectively.

To compare the results of the three stainless steels, the TTS and CCS diagrams for these alloys for different degrees of CW ranging from 0% to 25% are collectively presented together in Figs. 3 and 4, respectively. From the TTS diagrams established for these three alloys with different degrees of CW, CCRs above which there is no risk of sensitization were also calculated using the method described elsewhere [1]. The results obtained are given in Table 2. Minimum time required for sensitization at nose temperature (t_{min}) was determined from TTS diagrams and are presented in Table 3 for all the three alloys.

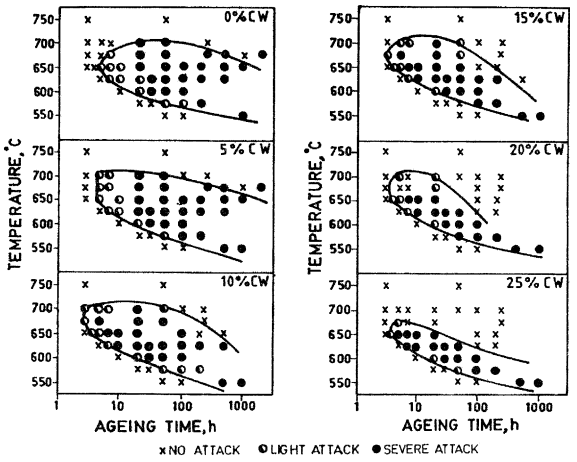

Fig. 1. TTS diagrams for AISI type 316 stainless steel (Alloy-2) with various degrees of CW established as per ASTM A262 practice E test.

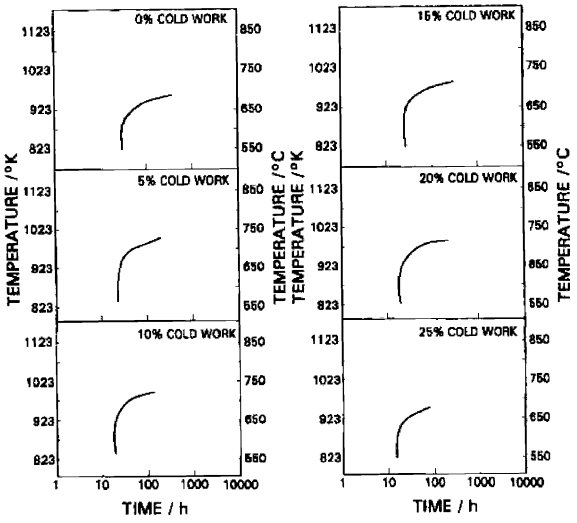

Fig. 2. CCS diagrams for AISI type 316 stainless steel (Alloy-2) with various degrees of CW.

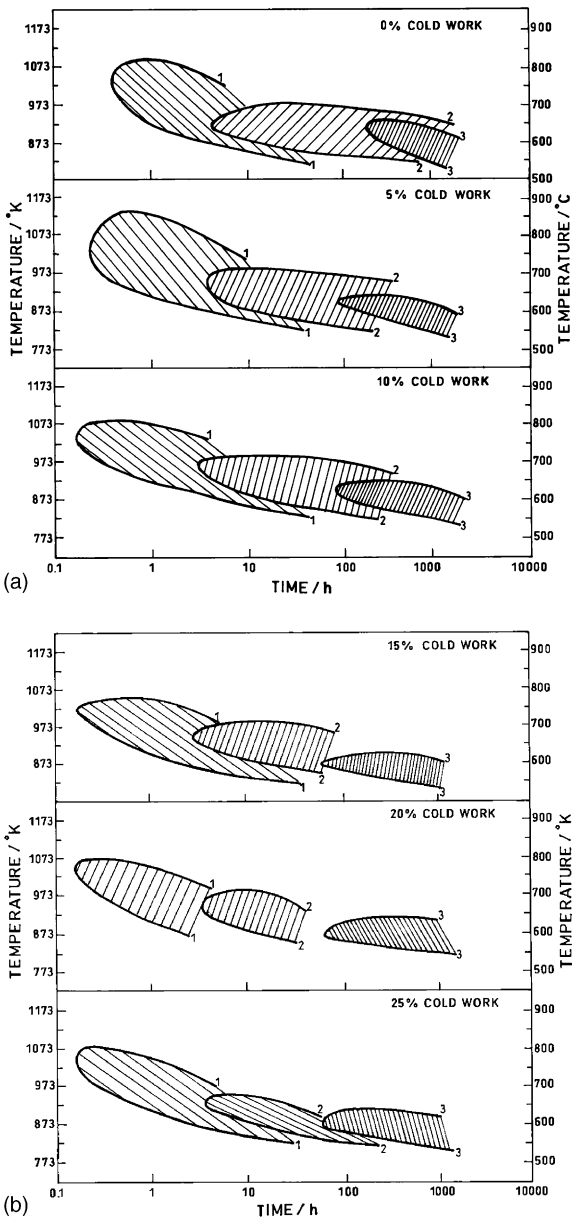

Fig. 3. TTS diagrams for AISI type 316 stainless steels with various degrees of CW established as per ASTM A262 practice E test: (1–1) Alloy-1; (2–2) Alloy-2; (3–3) Alloy-3 (hatched areas shows sensitized regions).

3.1. Influence of chemical composition

Sensitization of austenitic stainless steel requires the precipitation of chromium rich carbides along grain boundaries. Although carbon and chromium are the predominant compositional variables controlling sensitization kinetics, other alloying elements also influence it by altering carbon and chromium activity. However, in order to establish the influence of any one element on sensitization kinetics with certainty, one should have prepared model alloys by keeping the wt% of all other elements same and varying only that element whose influence has to be established. Although numerous literatures are available, in most of the studies variation in several elements are often found (with a few exceptions) which makes the interpretation of these results difficult.

It has been well-established that, by reducing the carbon content in stainless steel, TTS curve is displaced towards longer time because carbon concentration in austenite becomes insufficient to form chromium carbide

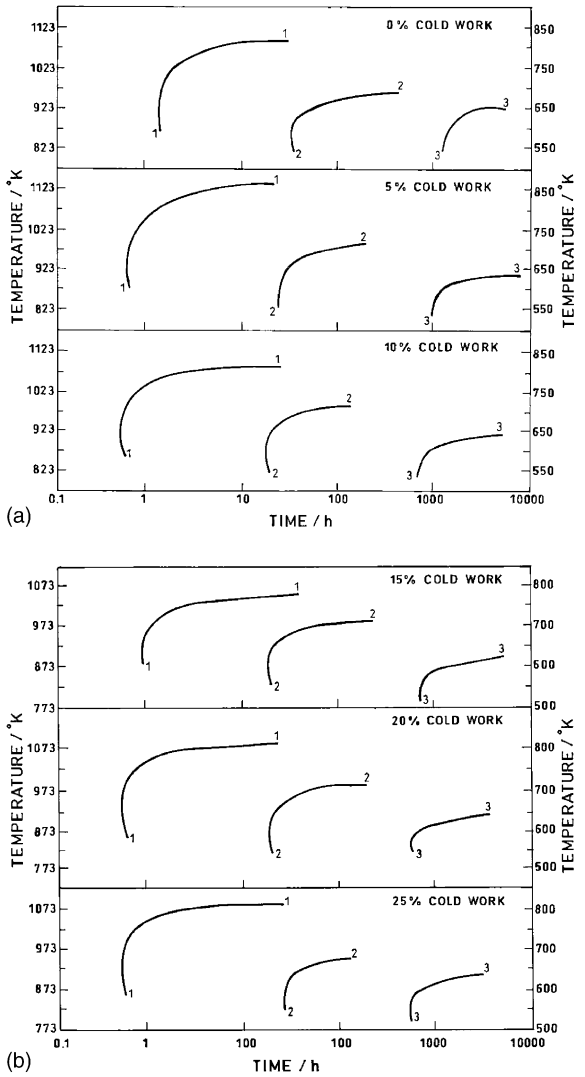

Fig. 4. CCS diagrams for AISI type 316 stainless steels with various degrees of CW: (1–1) Alloy-1; (2–2) Alloy-2; (3–3) Alloy-3.

Table 2
Critical linear cooling rate (K/h)

%CW	Alloy-1	Alloy-2	Alloy-3
0	365	17	0.43
5	710	22	0.54
10	765	27	0.73
15	515	27	0.76
20	815	26	0.93
25	790	18	0.97

readily. The limit of carbon content for which a steel is not susceptible to sensitization is closely connected with the presence of other alloying elements like chromium, molybdenum, nickel, nitrogen, manganese, boron, silicon as well as titanium and niobium in stabilized steels. Chromium has a pronounced effect on the passivation characteristics of stainless steel. With higher chromium contents, time to reach the resistance limit of chromium depletion at the grain boundaries is shifted to longer time. Alloys with higher chromium contents will be more resistant to sensitization.

Nickel is required in austenitic stainless steel to stabilise the austenitic phase and must be increased with increasing chromium concentration. Increasing the bulk nickel content decreases the solubility and increases the diffusivity of carbon. This effect is much more pronounced when nickel content is greater than 20%. It is generally recommended that in 25/20 Cr–Ni steel, carbon content should be less than 0.02% to guarantee resistance to sensitization [7]. Molybdenum reduces the solubility of carbon in austenite. Carbide precipitation is accelerated at higher temperatures whereas at lower temperatures it is slowed down [7]. When molybdenum is present, it is also incorporated in $M_{23}C_6$. Therefore in addition to chromium depletion, molybdenum depletion is also revealed. In molybdenum containing austenitic stainless steels $(Fe,Cr)_{23}C_6$ is precipitated first at 1023–1123 K. With prolonged aging molybdenum is also incorporated as $(Fe,Cr)_2Mo_2C_6$ which is finally converted to Chi (χ) phase. With increasing molybdenum contents, $M_{23}C_6$ precipitation and sensitization becomes increasingly influenced by the precipitation of intermetallic phases.

The influence of manganese is of special importance because in fully austenitic welds this element is added. Manganese reduces the carbon activity and increases its solubility. Carbide precipitation is slowed down and hence it appears to inhibit carbide precipitation [2]. Boron retards the precipitation of chromium carbide but depending upon the heat treatment it promotes sensitization [8]. Silicon promotes sensitization of high purity and commercial stainless steels [9,10]. Steels containing molybdenum were found to be much more sensitive to silicon addition. The increased susceptibility to sensitization in highly oxidizing solution is due to the segregation of silicon to grain boundaries. Apart from $M_{23}C_6$, 'Pi' phase which is a carbonitride is precipitated with increasing silicon contents. $M_{23}C_6$ precipitation is slowed down more and is substituted by Pi phase $(M_{11}(CN)_2)$. The cause for its precipitation seems to be the simultaneous effect of silicon on carbon and nitrogen activity. The influence of nitrogen on sensitization kinetics is quite complex and is dependent on the presence of other alloying additions. Nitrogen content up to 0.16 wt% is reported to improve sensitization resistance by retarding the precipitation and growth of $Cr_{23}C_6$ [11]. The detrimental effect of carbon on sensitization can be reduced by the addition of stabilizing elements like titanium and niobium.

Table 3
Variation of t_{min} with degree of CW

%CW	Alloy-1		Alloy-2		Alloy-3	
	Temperature (K)	t_{min} (h)	Temperature (K)	t_{min} (h)	Temperature (K)	t_{min} (h)
0	1053–1033	0.42	923	4.4	913	185
5	1023	0.25	973–923	4.5	903	94
10	1023	0.16	973–953	3	903	83
15	1023	0.17	943	2.8	873	60
20	1023	0.17	953	3.3	873	60
25	1063–1023	0.17	953	3.6	873	63

In order to predict a materials propensity to sensitization from its bulk composition, the effect of each element on the local chromium depletion and on the local dissolution/passivation characteristics must be known. Since this type of information is not available, composition effects are predicted empirically through correlation to sensitization.

Based on the numerous data reported in literature by various investigators, several attempts were made to predict time required for sensitization using composition-based correlation. Those elements which have major influence on kinetics of sensitization are given proper weightage and effective chromium content (Cr^{eff}) was calculated. One concept which has proven useful to take into account the variation is that of effective chromium content originated by Cihal [12] and has been fully developed by Fullman [13]. The central idea in this model is that the important variable in determining the time required for sensitization is the local chromium activity at the interface between the growing carbide and the matrix immediately after the carbide is precipitated. As this activity decreases the time required to produce a sensitized microstructure should decrease. The chromium activity at this interface will depend not only on the chromium concentration in the alloy but also on the concentration of other elements. The effective chromium content (Cr^{eff}) that one calculates is reflection of this change in the chromium activity produced by other elements. The effective chromium content should not be taken as a true composition. When this Cr^{eff} decreases, sensitization occurs rapidly. Cihal [12] rationalized heat to heat variability in IGC and stress corrosion cracking resistance by normalising compositional differences with effective chromium and carbon concentrations.

$$Cr^{eff} = Cr + (1.0\text{–}1.7)Mo - 100C - 0.2Ni + 2. \quad (1)$$

According to Fullman [13], susceptibility of an alloy to IGSCC could be judged by chromium concentration in equilibrium with $M_{23}C_6$ type carbide. Individual alloying elements were then assessed by considering their effect on several factors including carbide formation and carbon activity and ultimately the equilibrium chromium concentration adjacent to the carbide. Fullman's equation is a significant contribution consisting of generation of chromium equivalency parameters for many additional elements present in stainless steels. Clark et al. [14] used TTS data to determine the effect of nitrogen, phosphorous and boron. Combining various data from Fullman [13], Clark et al. [14] and Binder et al. [15], chromium equivalency parameter for nitrogen, Cr^{eff} can be calculated as follows:

$$\begin{aligned} Cr^{eff} = {} & Cr + 1.45Mo - 0.19Ni - 100C + 0.13Mn \\ & - 0.22Si - 0.51Al - 0.20Co + 0.01Cu \\ & + 0.61Ti + 0.34V - 0.22W + 9.2N. \end{aligned} \quad (2)$$

These empirical equations are generally used by other investigators for computing time required for sensitization whereas the Cr^{eff} concept is utilized here to explain the sensitization kinetics. As seen from the composition (Table 1), Alloy-1 contains 0.054% carbon and 0.053% nitrogen whereas Alloy-2 contains 0.043% carbon and 0.075% nitrogen. Alloy-3 contains 0.03% carbon and 0.086% nitrogen. In addition to these two elements, all other elements which can cause significant variations in solubility and activity of carbon and chromium also show minor variations. Based on Eq. (2), Cr^{eff} was calculated for all the three alloys under investigation and was found to be 12.57, 14.36 and 16.03 for Alloy-1, Alloy-2 and Alloy-3, respectively. For all these three alloys, time–temperature combinations leading to chromium carbide precipitation (ditch structure) was determined by performing ASTM A262 practice A test. Using the results, time–temperature-precipitation diagram for Alloy-3 has been reported [5] earlier. It was found that increasing Cr^{eff} does not have significant influence on the area of $M_{23}C_6$ precipitation in these three austenitic stainless steels. However variations in Cr^{eff} is found to exert a strong influence on sensitization susceptibility. When Cr^{eff} was 12.57, t_{min} for Alloy-1 at 0% CW was 0.42 h. When it increases to 14.36 (Alloy-2), t_{min} was 4.5 h. With further increase in Cr^{eff} to 16.03 for Alloy-3, t_{min} was shifted to 185 h. These data clearly indicate that with higher Cr^{eff}, the time to reach the resistance limit of chromium depletion at the grain boundaries is shifted to longer periods of time. The

upper boundary temperature progressively decreases with increase in Cr^{eff} (from 1073 K for Alloy-1, about 973 K for Alloy-2 and 923 K for Alloy-3). This can be attributed to the fact that higher chromium content facilitates the diffusion of chromium into the depleted grain boundary areas. This produces a shift of the upper boundary of the area of sensitization towards lower temperatures. Increase in Cr^{eff} results in shifting of the onset of sensitization to longer durations. Area which is prone to sensitization is also narrowed.

From these results it can be concluded that kinetics of sensitization vary by several orders of magnitude for these three alloys for each degree of CW. However this behaviour cannot be totally attributed to carbon and nitrogen alone because the wt% of other elements also show significant variations. The higher weightage given to carbon and nitrogen in the calculation of Cr^{eff} compared to those of other alloying elements adequately reflect their major role in influencing the sensitization kinetics.

Various views have been proposed by different authors to explain the effect of nitrogen on sensitization kinetics of stainless steel [2,11,16–22]. The computation of volume diffusion coefficient of chromium as a function of nitrogen indicates that nitrogen addition decreases the chromium diffusivity thereby retarding the nucleation and growth of carbides [16]. The systematic study using analytical electron microscopy was conducted by Briant et al. [2] for 304 stainless steel containing various amounts of nitrogen. They found that chromium concentration near the grain boundary is more and that the volume of the chromium depleted zone (considering both width and depth) decreases as the nitrogen content of the alloy increases. In addition, the solubility of nitrogen in austenite is greater than that of carbon. Another view is that in the presence of nitrogen, the passivation characteristics of the alloy is so superior that higher chromium depletion levels are necessary for sensitization [11]. In essence, nitrogen retards $M_{23}C_6$ precipitation by decreasing the diffusivity of Cr [23]. When the wt% of nitrogen is higher than 0.16 wt%, M_2N is formed. However, the kinetics of formation M_2N are very sluggish. Even if it forms the extent of chromium depletion around M_2N will be less compared to that of $M_{23}C_6$ because on mole per solute basis, less chromium is precipitated by nitrogen than by carbon.

3.2. Influence of prior deformation

From the TTS diagrams it can be seen that the nose of the C curve corresponding to the maximum rate of sensitization occurs at 1023 K for Alloy-1 in the 0% CW condition. As the degree of CW increases, nose temperature remains almost same but t_{min} decrease with increase in %CW up to 15% and thereafter remains constant. For Alloy-2 and Alloy-3, the TTS diagrams are shifted towards lesser time and lower temperatures than that of the 0% CW material. The nose temperature decreases with increase in CW up to 15% and above that remains almost the same. The upper boundary temperature for sensitization is lowered significantly with increase in CW.

Another important influence of CW is on desensitization of these stainless steels. For prolonged aging the sensitization effect is removed and the material shows no failures in the ASTM A262 practice E tests (Figs. 1 and 3). This phenomenon is known as desensitization and occurs due to the diffusion of chromium to the depleted region at the grain boundaries (homogenization). It is evident from Figs. 1 and 3 that the specimens become desensitized after aging for long time at high temperatures. The time required for desensitization at a given temperature also shows systematic trend with %CW as per the data shown in Table 4. As the %CW increases desensitization kinetics are faster and quicker homogenization takes place.

It can also be seen that as degree of CW increases, the CCR above which there is no risk of sensitization also increases because with increase in CW sensitization kinetics are faster and hence faster cooling rate must be used to avoid sensitization. For Alloy-3 containing 0.03% carbon and 0.086% nitrogen, the CCR varies from 0.43 to 0.97 K/h compared to 365–815 K/h for Alloy-1. Since the critical cooling rate is so low, sensitization in HAZ during welding is unlikely in Alloy-3.

All the above results reveal that the effect of CW on the sensitization kinetics is to enhance the rate of sensitization. Deformation of austenitic stainless steels results in lot of changes in the defect structure of the material. CW produces extensive dislocation networks and grain boundary ledges which allow rapid pipe diffusion of the chromium and faster nucleation of carbides. The enhanced kinetics of sensitization due to CW can be attributed to higher diffusivity of chromium and lower free energy barrier to carbide nucleation at grain boundaries in the deformed microstructure. The 0% CW material has a low dislocation density which increases sharply on cold working. It has been reported that with a small degree of CW there is a large increase in

Table 4
Variation of $t_{desen.}$ with %CW for Alloy-2

%CW	Time required for desensitization (h)			
	948 K	923 K	898 K	873 K
0	>1000	–	–	–
5	>1000	>1000	–	–
10	70	200	–	–
15	50	100	–	–
20	–	29	200	500
25	5	20	170	350

dislocation density at the grain boundaries which is higher than that of the matrix. The presence of such a defective structure containing dislocations, stacking faults etc. is known to enhance the overall diffusion of alloying elements and results in faster sensitization. At high levels of CW the nose temperature and the upper temperature boundary decreases which could be explained by the Hart dislocation pipe diffusion equation [24]

$$D_{\text{tot}} = D_{0,\text{l}}\mathrm{e}^{-Q_{\text{a}}/RT} + nAD_{0,\text{p}}\mathrm{e}^{-(Q_{\text{a,p}}/RT)}, \tag{3}$$

where D_{tot} is the total diffusivity, $D_{0,\text{l}}$ is the diffusion coefficient for lattice diffusion, $D_{0,\text{p}}$ the diffusion coefficient for pipe diffusion, Q_{a} the activation barrier for lattice diffusion, $Q_{\text{a,p}}$ the activation barrier for pipe diffusion, n the dislocation density, A the area of dislocation pipe, R the gas constant, T the temperature in Kelvin. When the degree of CW increases, n increases resulting in higher diffusivity of chromium. When the temperature is also high, the lattice diffusivity becomes very high and partial recovery from the CW effect sets in. Therefore, the effect of CW on the sensitization behaviour at high temperatures is less pronounced. Since stainless steels have a low stacking fault energy, high levels of CW results in large dislocation pileups on slip planes. Due to this, slip planes become additional favourable sites for carbide precipitation within the grain. This leads to short diffusion paths for carbon. Once the carbon activity is reduced, the chromium activity near the intragranular carbide precipitate increases due to quicker homogenization and the material no longer shows marked depletion of chromium at the grain boundaries and faster desensitization results.

3.3. Influence of prolonged thermal aging

Investigations were carried out to establish sensitization susceptibility of Alloy-2 after extensive aging beyond desensitization regime. Alloy-2 was aged at 898–973 K for various durations such as 500, 1000 and 2000 h. For these thermally aged specimens microstructural locations where $M_{23}C_6$ precipitation takes place both in as-received and cold worked material were determined by ASTM A 262 practice A test. Similarly practice E was also done to determine whether the materials are sensitized or desensitized. The results obtained in ASTM practice E test for the thermally aged specimens are presented in the TTS diagrams in Fig. 5.

Analysis of the results listed in Table 5 reveals when aged for 500 h, as the temperature increases, the extent of attack in E test decreases and at 898 K only very light attack was observed and at 973 K the material was totally immune. This indicates that as temperature increases replenishment of chromium in the depleted zone has set in and desensitization kinetics are faster at higher temperatures. Similarly when degree of CW increases

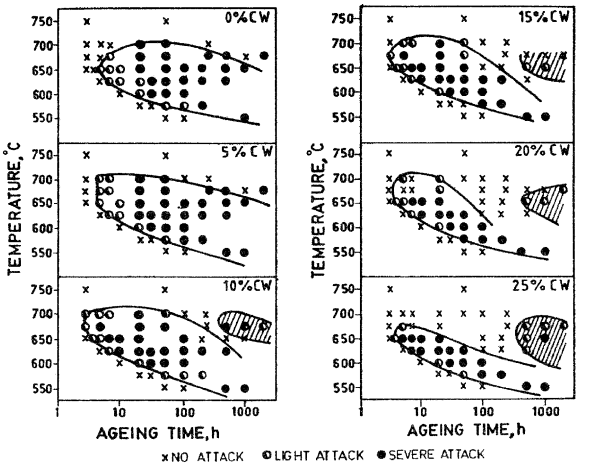

Fig. 5. TTS diagrams for AISI type 316 stainless steel (Alloy-2) with various degrees of CW established as per ASTM A262 practice E test (hatched areas show regions of precipitation of secondary phases).

desensitization kinetics are faster. But the most important observation is that when the desensitized specimens were aged further, for example for 2000 h, they failed in the practice E test with very severe attack. In order to confirm whether this is due to IGC attack, the thermally aged material was subjected to 'U'-bend test and it was found that even before exposure to E test, the material failed due to reduction in ductility.

From the EPR data presented in Table 5 it can be clearly seen that for a given heat treatment as the degree of CW increases, Q value decreases indicating that the extent of alloy (Cr/Mo) depletion decreases which implies that 'desensitization' has set in. Similar decrease in Q was observed when aging time increases for any particular CW. In other words both increase in degree of CW and increase in aging time resulted in lower Q values indicating homogenization of depleted zone and onset of desensitization.

The XRD patterns were thoroughly analyzed and the phases identified are collectively presented in Table 5. From these data, it can be found that several secondary phases such as χ, Laves (η), σ and carbonitrides start precipitating due elevated temperature aging. Since they are embrittling phases, they result in reduction in ductility. To ensure that these phases embrittle in the as-aged condition itself, specimen were subjected to U-bend test without exposing to practice 'E' test and all the specimens which failed in E test failed in as-aged condition itself. This implies sensitization due to chromium depletion is not the cause for failure but the formation of embrittling secondary phases is responsible for the reduction in ductility. All these observations can be summarised as follows.

Table 5
Results obtained for cold worked and thermally aged Alloy-2 in ASTM A262A, E and EPR tests

Heat treatment	Results obtained in			Secondary phases present
	A262A	A262E	EPR (Q) mC/cm^2	
898 K–500 h–0% CW	Ditch	Failed	543.2 ± 23.0	$M_{23}C_6$
898 K–500 h–5% CW	Ditch	Failed	529.5 ± 23.3	$M_{23}C_6$
898 K–500 h–10% CW	Ditch	Failed	435.6 ± 6.1	$M_{23}C_6$
898 K–500 h–15% CW	Ditch	Passed	74.3 ± 5.3	$M_{23}C_6$
898 K–500 h–20% CW	DMP	Passed	40.2 ± 1.0	$M_{23}C_6$
898 K–500 h–25% CW	DMP	Failed	19.3 ± 0.9	Not analysed
923 K–500 h–0% CW	Ditch	Failed	379.9 ± 13.4	$M_{23}C_6$, χ, η
923 K–500 h–5% CW	Ditch	Failed	535.9 ± 5.6	–
923 K–500 h–10% CW	Ditch	Passed	48.0 ± 2.8	–
923 K–500 h–15% CW	Ditch	Passed	16.9 ± 4.2	–
923 K–500 h–20% CW	DMP	Failed	5.4 ± 0.5	–
923 K–500 h–25% CW	DMP	Failed	3.6 ± 1.7	$M_{23}C_6$, χ, η, carbonitrides
923 K–1000 h–0% CW	Ditch	Failed (LA)	303.4 ± 37.7	$M_{23}C_6$, χ, η, carbonitrides
923 K–1000 h–5% CW	Ditch	Failed (LA)	98.8 ± 6.5	–
923 K–1000 h–10% CW	DMP	Failed (LA)	4.7 ± 2.1	–
923 K–1000 h–15% CW	DMP	Failed	5.2 ± 1.6	–
923 K–1000 h–20% CW	DMP	Failed	4.1 ± 1.5	–
923 K–1000 h–25% CW	DMP	Failed	6.2 ± 1.5	$M_{23}C_6$, χ, η, carbonitrides
923 K–2000 h–0% CW	Ditch	–	81.4 ± 3.8	$M_{23}C_6$, χ, η
923 K–2000 h–5% CW	Ditch	–	22.4 ± 1.2	–
923 K–2000 h–10% CW	DMP	–	24.7 ± 4.2	–
923 K–2000 h–15% CW	DMP	–	11.8 ± 5.1	–
923 K–2000 h–20% CW	DMP	–	3.9 ± 1.6	–
923 K–2000 h–25% CW	DMP	–	8.1 ± 2.6	$M_{23}C_6$, χ, η, carbonitrides
948 K–500 h–0% CW	Ditch	Failed (LA)	193.1 ± 5.1	$M_{23}C_6$, χ
948 K–500 h–5% CW	Ditch	Failed (LA)	11.9 ± 6.3	–
948 K–500 h–10% CW	DMP	Failed (LA)	19.9 ± 2.8	–
948 K–500 h–15% CW	DMP	Passed	4.4 ± 0.8	–
948 K–500 h–20% CW	DMP	Failed (LA)	4.6 ± 2.2	–
948 K–500 h–25% CW	DMP	Failed LA)	3.3 ± 1.0	$M_{23}C_6$, χ, η
948 K–1000 h–0% CW	Ditch	Failed (LA)	6.8 ± 3.5	$M_{23}C_6$, χ, σ
948 K–1000 h–5% CW	Ditch	Failed (LA)	18.1 ± 3.4	–
948 K–1000 h–10% CW	Ditch	Failed (LA)	5.4 ± 1.8	–
948 K–1000 h–15% CW	DMP	Failed	36.4 ± 10.0	–
948 K–1000 h–20% CW	DMP	Failed	1.7 ± 0.6	–
948 K–1000 h–25% CW	DMP	Failed	2.2 ± 0.8	$M_{23}C_6$, χ, η, carbonitrides
948 K–2000 h–0% CW	Ditch	–	4.8 ± 2.2	$M_{23}C_6$, χ, σ, η
948 K–2000 h–5% CW	Ditch	–	1.7 ± 0.8	–
948 K–2000 h–10% CW	Ditch	–	1.9 ± 1.2	–
948 K–2000 h–15% CW	DMP	–	2 ± 0.9	–
948 K–2000 h–20% CW	DMP	–	1.6 ± 0.9	–
948 K–2000 h–25% CW	DMP	–	3.2 ± 1.2	$M_{23}C_6$, χ, σ, η
973 K–500 h–0% CW	Ditch	Passed	0.5[a]	$M_{23}C_6$, χ, η, carbonitrides
973 K–500 h–5% CW	Ditch	Passed	2.1[a]	$M_{23}C_6$
973 K–500 h–10% CW	Ditch	Passed	0.6[a]	$M_{23}C_6$
973 K–500 h–20% CW	DMP	Passed	3.1 ± 1.2	$M_{23}C_6$
973 K–500 h–25% CW	DMP	Passed	–	$M_{23}C_6$, χ, η

DMP – ditch structure with matrix precipitation.
LA – light attack.
[a] Data from single test.

When austenitic stainless steels are thermally aged $M_{23}C_6$ precipitates successively on grain boundaries, incoherent twin boundaries, coherent twin boundaries and finally intragranularly within the matrix. Since the formation of other secondary phases involves diffusion of bulky elements like Fe and Mo these are observed only after aging for 2000 h. Moreover, carbon in solid solution prevents the formation of σ phase because of its inability to dissolve carbon and hence σ is observed only when $M_{23}C_6$ precipitation is complete and matrix carbon level decreases whereas χ, η are observed simultaneously with $M_{23}C_6$. Since no attempt was made in this investigation to quantitatively estimate each individual phase, the influence of CW on growth kinetics cannot be interpreted from the XRD patterns. But with fair amount of certainty it can be concluded that as CW level increases, newer phases are formed and ductility gets drastically reduced. This may be attributed to the enhanced diffusion of alloying elements due to the defects introduced by cold working.

Hence, prolonged thermal aging of the investigated type 316 stainless steels containing 760 ppm nitrogen at elevated temperature results in the formation of χ, Laves, σ phases in addition to carbonitrides and this reduces the ductility of this alloy and leads to embrittlement in service. CW accelerates precipitation and growth kinetics of these phases.

4. Conclusions

The sensitization behaviour of AISI 316 stainless steels having different chemical composition was studied for various degrees of CW ranging from 0% (mill-annealed) to 25% reduction in thickness. From the results obtained TTS and CCS diagrams were constructed. Using these data, the CCR was calculated above which there is no risk of sensitization during continuous cooling. When TTS diagrams and CCS diagrams for these three stainless steels were collectively presented in one diagram for the various CW level, several systematic trends were observed with respect to chemical composition. Although carbon and nitrogen are the elements influencing sensitization kinetics predominantly, the role of other elements are also taken into consideration by computing Cr^{eff} from composition based correlation. It was found that as Cr^{eff} increases, upper boundary temperature for sensitization is lowered, area prone to sensitization is reduced and time required for onset of sensitization is increased. It has been established that cold working up to 15% accelerates the sensitization kinetics and on further cold working there is not much difference in the sensitization kinetics; however desensitization kinetics are very fast at higher levels of CW especially at high temperatures. When one of the stainless steels is thermally aged for long duration for time periods exceeding those required for desensitization, precipitation of secondary phases such as chi (χ), sigma (σ), carbonitride and Laves phases sets in which deteriorate the ductility of the material. Hence such material fail in ASTM practice E test. EPR tests are useful to analyse the data. Prior deformation enhances precipitation and growth kinetics. The systematic trend observed in these experimentally determined sensitization data on these three steels would eliminate the need for independent generation of TTS and CCS diagrams for any stainless steel whose composition lies within the range specified in this investigation. The database reported here will help to recommend the limits of critical cooling rate to avoid sensitization during fabrication.

Acknowledgements

The authors are grateful to Dr Baldev Raj, Director, Metallurgy, Chemistry and Reprocessing Group, Dr V.S. Raghunathan, Associate Director, Materials Characterisation Group, Dr H.S. Khatak, Head, Corrosion Science and Technology Division, Indira Gandhi Centre for Atomic Research, Kalpakkam for their keen interest and support during the course of this investigation. The authors gratefully acknowledge the assistance provided by Smt K. Parimala in carrying out the heat treatments and IGC tests. The authors are thankful to Shri K. Thyagarajan for his help in preparing the drawings.

References

[1] R.K. Dayal, J.B. Gnanamoorthy, Corrosion 36 (1980) 104.
[2] C.L. Briant, R.A. Mulford, E.L. Hall, Corrosion 38 (1982) 468.
[3] S.K. Mannan, R.K. Dayal, M. Vijayalakshmi, N. Parvathavarthini, J. Nucl. Mater. 126 (1984) 1.
[4] N. Parvathavarthini, R.K. Dayal, S.K. Seshadri, J.B. Gnanamoorthy, J. Nucl. Mater. 168 (1989) 83.
[5] N. Parvathavarthini, R.K. Dayal, J.B. Gnanamoorthy, J. Nucl. Mater. 208 (1994) 251.
[6] Annual Book of ASTM Standards, ASTM, Philadelphia, PA, 1991, vol. 03.02.
[7] E. Folkhard, in: Welding Metallurgy of Stainless Steels, Springer, Vienna, 1988.
[8] R.A. Lula, A.J. Lena, G.G. Kiefer, Trans. Am. Soc. Met. 46 (1954) 197.
[9] J.S. Armijo, Corrosion 24 (1968) 24.
[10] A. Joshi, D.J. Stein, Corrosion 28 (1972) 321.
[11] T.A. Mozhi, W.A.T. Clark, K. Nishimoto, W.B. John, D.D. McDonald, Corroision 41 (1985) 555.
[12] V. Cihal, Inter granular corrosion of Cr–Ni stainless steel, Unieux conference, 5 May 1969.
[13] R.L. Fullman, Acta Metall. 30 (1982) 1407.
[14] W.A.T. Clark, T. Arul Mozhi, D.D. MacDonald, DOE/ER/10972-T2, April 1983.

[15] W.O. Binder, C.M. Brown, R. Franks, Trans. ASM 41 (1949) 1301.
[16] H.S. Betrabet, K. Nishimoto, B.E. Wilde, W.A.T. Clark, Corrosion 43 (1987) 77.
[17] J.J. Eckenrod, C.W. Kouach, in: C.R. Brinkman, H.W. Garvin (Eds.), Effect of Nitrogen on the Sensitization, Corrosion and Mechanical Properties of 18Cr-8Ni SS, ASTM-STP 679, ASTM, Philadelphia, PA, 1979, p. 17.
[18] A. Kendal, J.E. Truman, K.B. Lomax, in: J. Foct, A. Hendry (Eds.), International Conference on High Nitrogen Steel, HNS-88, Lille, 1988, Institute of Metals, York, 1989, p. 405.
[19] P. Gumpel, T. Ladwein, in: J. Foct, A. Hendry (Eds.), International Conference on High Nitrogen Steel, HNS-88, Lille, 1988, Institute of Metals, York, 1989, p. 272.
[20] J.E. Truman, in: J. Foct, A. Hendry (Eds.), International Conference on High Nitrogen steel, HNS-88, Lille, 1988, Institute of Metals, York, 1989, p. 225.
[21] R.F.A. Jargelius, Effect of nitrogen alloying on sensitization behaviour of two highly alloyed austenitic stainless steels, in: International Conference on Stainless Steel 87, Institute of Metals, York, 1987, p. 266.
[22] R.S. Dutta, P.K. De, H.S. Gadiyar, Corros. Sci. 34 (1995) 51.
[23] P. Marshall, in: Austenitic Stainless Steels: Microstructure and Mechanical Properties, Elsevier Applied Science, London, 1984, p. 23.
[24] A.H. Advani, L.E. Murr, D.G. Atteridge, R. Chelakara, Metall. Trans. 22A (1991) 2917.